Divergent climate feedbacks on ~~in~~ winter wheat ~~the~~ growing ~~period~~ and ~~the~~ dormancy periods ~~to~~ as affected by sowing date ~~shift of winter wheat~~ in the North China Plain

Fengshan Liu[1,2], Ying Chen[1,*], Nini Bai[1], Dengpan Xiao[4], Huizi Bai[4], Fulu Tao[2,3,5], Quansheng Ge[2,3]

1. China National Engineering Research Center of JUNCAO Technology, Forestry College, Fujian Agriculture and Forestry University, Fuzhou 350002, China
2. Key Laboratory of Land Surface Pattern and Simulation, Institute of Geographic Sciences and Natural Resources Research, CAS, Beijing 100101, China;
3. College of Resources and Environment, University of Chinese Academy of Sciences, Beijing 100049, China
4. Institute of Geographical Sciences, Hebei Academy of Sciences, Shijiazhuang 050011, China
~~4.~~5. Natural Resources Institute Finland (Luke), Helsinki 00790, Finland

Author: Liu Fengshan, PhD, specialized in agricultural meteorology and regional climate change. E-mail: liufs.11b@ igsnrr.ac.cn

* Corresponding author

Abstracts: Crop phenology exerts measurable impacts on soil surface properties, biophysical processes, and climate feedbacks, particularly at local/regional scales. ~~The land cover and management changes have strong feedbacks to climate through surface biophysical and biochemical processes. Agricultural phenology dynamic exerted~~

带格式的: 字体: (默认) Times New Roman, 小四

带格式的: 字体: (默认) Times New Roman, 小四

~~measurable impacts on land surface properties, biophysical process and climate feedback in particular times at local/regional scale.~~ Nevertheless, the response of surface biophysical processes to climate feedbacks as affected by sowing date in winter wheat croplands has been overlooked, especially during winter dormancy~~But the responses of climate feedback through surface biophysical process to sowing date shift in the winter wheat ecosystem have been overlooked, especially at winter dormancy period~~. The dynamics of leaf area index (LAI), surface energy balance and canopy temperature (T_c) were simulated by modified SiBcrop model under two sowing date scenarios (Early Sowing: EP; Late Sowing: LP) at 10 stations in the North China Plain. The results showed that the SiBcrop with a modified crop phenology scheme ~~better~~ well simulated the seasonal dynamic of LAI, T_c, phenology, and surface heat fluxes. Earlier sowing date had higher LAI with earlier development than later sowing date. But the response of T_c to sowing date exhibited opposite patterns during the dormancy and active growth periods: EP led to higher T_c (0.05 K) than LP in the dormancy period and lower T_c (-0.2K) in the growth period. The highest difference (0.6 K) between EP and LP happened at the time when wheat was sown in EP but wasn't in LP. The higher LAI captured more net radiation with ~~lower surface albedo for~~ warming effect, ~~whist~~ but partitioned more energy into latent heat flux with~~surface energy partitioning exerted~~ cooling ~~effect~~. The climate feedback of sowing date, which was more obvious in winter in the northern areas and in the growing period in the southern areas, was determined by the~~The~~ relative contributions of albedo-radiative process and partitioning-non-radiative process. ~~determined the climate effect of sowing date shift. The spatial pattern of the climate~~

带格式的: 字体: (默认) Times New Roman, 小四

带格式的: 字体: (默认) Times New Roman, 小四

带格式的: 字体: (默认) Times New Roman, 小四

~~response to sowing date was influence by precipitation and air temperature.~~ The study climate. ~~climate effects of the sowing date shift in winter dormancy period are worthy~~

Key words: sowing date, canopy temperature, phenology, leaf area index, winter wheat, land surface model, North China Plain

1. Introduction

Land-atmosphere interactions are key components of the climate system. The land cover and management changes have strong feedbacks with climate through surface biophysical and biochemical processes (Mahmood et al. 2014). Cropland surface characteristic had been and will continue to be changed through ~~agricultural~~ crop management, such as cropping system (Jeong et al. 2014; Cui et al. 2018), sowing date and phenology shifts (Sacks et al. 2011; Richardson et al. 2013), and cultivars selection~~bio-geoengineering~~ (Seneviratne et al. 2018), to keep high yield under climate change condition. The changed cropland~~surface~~ properties ~~in farmland~~ further generate feedback to regional climate through surface energy partitioning and albedo (α) mechanisms (Cooley et al. 2005; Zhang et al. 2015). It is important to quantify the climate feedback of crop phenology ~~shift~~ for regional climate prediction and agriculture sustainable development.

There are evidences that crop phenology has been ~~shifts~~ shifted substantially in the major cultivation areas worldwide (Sacks and Kucharik 2011; Tao et al. 2012; Tao et al. 2014; Liu et al. 2017). In the North China Plain (NCP), the dates of ~~seeding~~sowing, dormancy, re-greening~~green up~~, anthesis, and maturity in wheat system were changed by 1.5, 1.5, -1.1, -2.7, and -1.4 days/decade (a positive value indicates delay and a negative value indicates advance), respectively (Xiao et al. 2013). The vegetative stages (including periods from dormancy to ~~greenup~~re-greening, re-greening~~greenup~~ to anthesis) ~~was~~ were shortened and reproductive stage was prolonged (Xiao et al. 2013). ~~The main contributors including climate change and crop management.~~ Global warming induced-higher temperature resulted in longer photosynthetic-active period but faster

带格式的: 字体: (默认) Times New Roman, 小四

development rate and shorter growth stages. Crop management, including sowing date adjustment and varietal change, reduced the length~~s~~ of vegetative stage, but increased the length of reproductive stage (Liu et al. 2010; Liu et al. 2018). The management induced phenology ~~change~~ dynamics ~~is~~ are intended to increase yield~~beneficial for high yielding~~. The strategies adapting to warmer environment include adopting cultivars with higher accumulated growing degree days (GDD) and later planting. The prolonged grain-filling period of winter wheat benefits the accumulation of carbohydrates ~~organic matter~~ in grain (Reynolds et al. 2012; Liu et al. 2018), and the adjusted sowing date reduces the risks such as insect and viral infection, adverse meteorological conditions, and soil water depletion ~~, et al.~~(Sacks et al. 2010). Model simulation indicated that yield increase of winter wheat was benefitted from cultivars renewal by 12.2-22.6% and fertilization management by 2.1-3.6%; climate change damaged yield by -15.0% for rain-fed type, in the NCP (Xiao et al. 2014).

The crop phenology ~~shifts change~~ affects the seasonal rhythm ~~of crop development and affect the~~of surface greenness ~~coverage of land surface~~ and energy and water exchanges in the boundary layer. For example, maize growth duration prolonged and reached maturity and senesced a couple of weeks later, and the maximum change can reach 47 W m^{-2} and -20 W m^{-2} for latent heat flux (*LH*) and sensible heat flux (*SH*), respectively, when the NDVI is increased by 0.1 in the Agro-IBIS model (Bagley et al. 2015). Earlier planting date and longer grain-filling period increased ~~(decreased)~~ the *LH* ~~(*SH*)~~ by ~~0.3 (0.2)~~3 W m^{-2}, decreased *SH* by 2.5 W m^{-2} ~~mm/year~~ in June and enhanced the net radiation (R_n) by 1.2 W m^{-2} in October by reducing the interval time from maturity to harvest in American ~~maize~~ Corn belt (Sacks and Kucharik 2011). The change of surface

带格式的: 字体: (默认) Times New Roman, 小四

带格式的: 上标

带格式的: 字体: 倾斜

coverage also shows a certainn regional climate feedback. The increased spring surface greenness at farmland, due to the advanced re-greening stage of winter wheat (Xiao et al. 2013; Liu et al. 2017), significantly impacted the patterns of *LH* and *SH* and then the changes of moderate to light rainfall (Zhang et al. 2015). Harvest shifted the key influence factors of the radiative balance and evaporative fraction from leaf area and soil-atmosphere temperature difference to soil moisture in U.S. winter wheat (Bagley et al. 2017), and a shift in radiative forcing with the potential to warm the atmosphere bywarming future atmosphere by 1~1.4 ℃ through decreasing declining *LH*evapotranspiration in the NCP (Cho et al. 2014). So, tThe influence of phenology on climate feedback through surface biophysical process at local/regional scale is worthy of further studies (Liu et al. 2017).

带格式的：字体：倾斜

Despite previous studies showed the critical role of crop phenology dynamic to in surface energy and water balance, there is an important potential sensitive period that has been ignored in the winter wheat system. During the dormancy period in winter, aboveground canopy of winter wheat remained constant for more than 2 months (Xiao et al. 2013). In view of the close relationships between surface biophysical processes and aboveground canopysurface characteristic (Boisier et al. 2012; Chen et al. 2015; Liu et al. 2017), the length from sowing date to start of dormancy would be the determinant factor to surface biophysical process in winter where winter wheat wildly widely distributed, such as NCP, Pacific Northwest (Wuest 2010) and Southern Great Plains of USA (Bagley et al. 2017)，Australia, and numerous countries surrounding the Mediterranean Sea (Mahdi et al. 1998; Schillinger 2011). Compared with climate feedback of other phenology dynamics, such as earlier re-greening stage (Xiao et al. 2013; Zhang et al.

2013), longer reproductive period (Sacks and Kucharik 2011) and inter-cropping period (Cho et al. 2014; Bagley et al. 2017), the climate feedback of sowing date emerges gradually with crop development. Particularly, winter wheat grows faster in early stage and slower as winter approaches, smaller change in sowing date could lead to larger and longer climate feedback in dormancy period. ~~the effects of sowing date on land surface characteristic in dormancy period of winter wheat and other winter crops are relatively indirect and the effects last longer.~~ Recognition of the impacts of sowing date on land surface characteristics and climate feedback would be beneficial to the understanding of human influence on climate change. Therefore, it is necessary to investigate whether dormancy period of winter wheat is sensitive to sowing date. And ~~if so,~~ how sensitivities are surface biophysical process and climate effect?

2. Data and methods

2.1. Study stations

The NCP, with an area of 4×10^5 km^2, is the largest winter wheat production region in China, including Hebei, Henan, Shandong, Jiangsu, and Anhui provinces, and Beijing and Tianjin municipalities (Fig.1). Summer maize - winter wheat rotation is the main cropping system~~, —~~, except Anhui and Jiangsu where winter wheat-rice rotation system is dominated. The satellite data showed a high cropland density above 70% with flat and relatively homogeneous agricultural practices (Liu et al. 2005; Ho et al. 2012). The soil type is classified as sandy loam according to the seven soil textures in the model (Sellers et al. 1996). Two stations with surface fluxes were used for model calibration (Fig.1, blue triangles). Ten randomly distributed stations with complete meteorology and phenology

带格式的: 字体: (默认) Times New Roman, 小四, 字体颜色: 自动设置, 图案: 清除

带格式的: 字体: (默认) Times New Roman, 小四, 字体颜色: 自动设置, 图案: 清除

带格式的: 上标

带格式的: 上标

带格式的: 字体: (默认) Times New Roman, 小四, 字体颜色: 自动设置, 图案: 清除

带格式的: 字体: (默认) Times New Roman, 小四, 字体颜色: 自动设置, 图案: 清除

带格式的: 字体: (默认) Times New Roman, 小四, 字体颜色: 自动设置, 图案: 清除

information were selected for simulation in this study (Fig.1, green dots). The details of fluxes, meteorology and phenology were further exhibited below.

~~with complete meteorology and phenology information were selected for this study (Fig.1, green dots). The natural conditions and agricultural production level of the selected stations are typical to the NCP. The stations maintain good records on both meteorological and winter wheat phenology data since 1981.~~

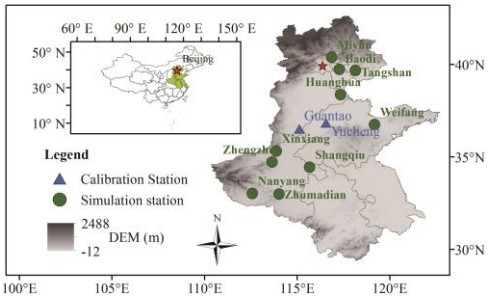

Fig.1 Distribution map of the study area and observation sites.

The 30 m resolution digital elevation model ~~(DEM)~~, provided by the GlobeLand30 in 2010, and the administrative map were downloaded from the National Catalogue Service For Geographic Information.

2.2 Data

2.2.1 Meteorology

The quality-controlled meteorological data, including air temperature (T_a), precipitation (P), atmosphere pressure, relative humidity, and wind speed, was obtained from the Chinese Meteorological Administration. Summer monsoon climate dominates the region with an uneven distribution of annual precipitation (Table 1). In the 1980-2012, the average annual P at the selected stations ranged between 550-990 mm, mainly happened in summer. The mean yearly T_a varied between 11-15 ℃. In the growing

season of winter wheat (11-12 and 1-6 month), the T_a varied between 7-11 ℃ among stations and P ranged between 170-420 mm, which is consistent with the average climatic conditions in the NCP (A et al. 2016). Climatological mean T_a and accumulated P during the wheat growth period were calculated in the 10 stations and were linearly regressed with the simulated differences between scenarios. Meteorological data was also used to drive the model. ~~Meteorological data was also used to drive the model in the selected 10 stations (Fig.1).~~

Table 1 Climate conditions of the selected stations in 1980-2012

	Station	Jan.	Feb.	Mar.	Apr.	May	Jun.	Jul.	Aug.	Sept.	Oct.	Nov.	Dec.	Average Wheat Season
T_a (℃)	Miyun	-5.9	-2.2	4.8	13.5	19.6	24	25.8	24.5	19.3	12	3	-3.7	6.6
	Baodi	-5	-1.4	5.3	13.6	19.5	24	26.1	24.8	19.8	12.7	3.7	-2.7	7.1
	Tangshan	-4.8	-1.3	5.1	13.4	19.4	23.7	25.9	25	20.3	13	4.1	-2.5	7.1
	Huanghua	-3.4	-0.2	5.9	14.1	20.3	25	26.9	25.8	21.2	14.2	5.5	-1.2	8.3
	Weifang	-2.8	0.1	5.8	13.2	19.2	23.9	26.2	25.2	20.7	14.4	6.4	-0.3	8.2
	Xinxiang	0	3.3	8.7	15.8	21.2	25.8	27	25.9	21.3	15.3	7.9	1.8	10.6
	Zhengzhou	0.5	3.5	8.7	16	21.5	26	27.1	25.7	21.2	15.5	8.4	2.5	10.9
	Shangqiu	0.1	3.1	8.3	15.1	20.6	25.4	26.9	25.7	21.1	15.3	8.1	2	10.3
	Nanyang	1.6	4.4	9.1	15.8	21.2	25.5	27	26	21.7	16.1	9.4	3.5	11.3
	Zhumadian	1.5	4.2	9	15.7	21.2	25.7	27.2	25.9	21.6	16.3	9.6	3.6	11.3
P (mm)	Miyun	2.2	4	9.7	19.9	43.1	86.7	180.7	172.6	62.9	25.5	9.4	2.3	177.3
	Baodi	2.7	3.7	9	20.1	36.2	82.4	169.7	142.6	49.7	27.5	10.1	3.6	167.8
	Tangshan	3.5	4.1	9.4	22.4	47	83.2	169.7	154.3	50.8	28.2	9.5	3.4	182.5
	Huanghua	3.2	5.5	10.1	21.3	42.8	84.2	177.2	111.6	41.5	31	11.9	3.5	182.5
	Weifang	6	10.3	14.9	24.5	45.4	80	136.5	132.1	56.1	32.8	18.8	8.9	208.8
	Xinxiang	4.6	7.1	19.2	25	49.9	65	150	119.5	59.8	32	14.9	5	190.7

带格式的：字体：(默认) Times New Roman，小四，字体颜色：自动设置，图案：清除

带格式的：字体：(默认) Times New Roman，小四，字体颜色：自动设置，图案：清除

带格式的：字体：倾斜

带格式的：字体：(默认) Times New Roman，小四，字体颜色：自动设置，图案：清除

带格式的：字体：(默认) Times New Roman，小四，字体颜色：自动设置，图案：清除

带格式的：字体：小四

Zhengzhou	9.6	12.4	27.1	30.9	63.6	67.8	146.6	134.7	75.6	40.5	21.1	9.1	241.6
Shangqiu	14.3	16.3	29.3	33	65	85.2	166.8	144.8	68.5	38.2	23.4	12.7	279.2
Nanyang	13.2	15.6	35.2	41.7	78.8	124.5	183.7	131.7	76.3	51.1	30	12.8	351.8
Zhumadian	21.9	24.8	51	50.9	93	128.6	227.7	176.3	98.2	63.9	35.2	18.5	423.9

T_a means air temperature, and P means precipitation.

2.2.2 Verification data

To verify the applicability of the model, surface flux data was collected from Yucheng and Guantao stations (Fig.1; Table 2). The two stations used the same eddy covariance instruments to measure the surface latent heat flux (LI7500, LI-COR Inc., Lincoln, NE, USA) and sensible heat flux (CSAT-3, Campbell Scientific Inc., Logan, UT, USA), but at different heights (Yucheng:3.3 m; Guantao: 15.6 m). The post-processing software (Yucheng: Eddypro; Guantao: EdiRe) was used to process the raw data such as spike detection, lag correction of H_2O/CO_2 relative to the vertical wind component, sonic virtual temperature correction, coordinating rotation using the planar fit method, corrections for density fluctuation (WPL-correction), and frequency response correction (Liu et al. 2011). The REddyProc was used for gap-filling by method of the look-up table and the mean diurnal variations method (Falge et al. 2001; Wutzler et al. 2018). More details could be refered to (Lei et al. 2010; Liu et al. 2013). Totally 10 complete winter wheat season flux data were used to validate the model (Table 2).

The meteorology conditions were also synchronously measured during flux observation (Table 2). The measurement included T_a, P, atmosphere pressure, relative humidity, wind speed, and sunshine. These data was the inputs of the model. According to the T_a and P, the meteorological conditions were similar between the 10 stations for simulation and the two stations for calibration. More variables were observed at Yucheng

station, such as wheat phenology and leaf area index (LAI) and canopy temperature (T_c). The observed durations of phenology, LAI, and fluxes at Yucheng station were in 2003-2006, 2004-2006, and 2003-2010, respectively.

Table 2 General information about model verification data

Station	Period	Wheat growing season T_a (~~K~~℃)	Wheat growing season P (mm)	Measured variables
Yucheng	2003-2010	~~282.15~~9	226.7	Meteorology, Phenology, LAI, *LH*, *SH*, T_c
Guantao	2008-2010	~~282.75~~9.6	134.4	Meteorology, *LH*, *SH*

T_a means air temperature, P means precipitation, LAI means leaf area index (m^2 m^{-2}), *LH* means latent heat flux (W m^{-2}), *SH* means sensible heat flux (W m^{-2}). T_c means the simulated canopy temperature (℃~~K~~).

2.2.3 Phenology of winter wheat

The phenology information was obtained from China agro-meteorological experiment stations~~manually recorded~~ and available in the period of 1981-2009, except for 2003 at Zhumadian and 1986 and 1988 at Miyun station (Table 3). Phenological statistics showed that the sowing time of winter wheat is generally between DOY (Day Of Year) 270-290 (early and middle October) in the NCP. After sowing, it generally takes about 6-10 days for germination. Winter wheat dormancy stage generally begins in DOY 330-360 (December) and ends in DOY 40-70 (late February and early March), and reaches maturity in DOY 150-160(mid-June). The standard deviation shows that the inter-annual fluctuations of dormant and re-greening period is larger, and harvest period is relatively stable.

For the past 30 years, winter wheat phenology at some stations showed a significant linear trend (Table 4). The sowing and germination periods were significantly delayed in 4 out of 10 stations, and the trend in the dormant and re-greening period was not obvious. Winter wheat matured significantly earlier at five stations. Generally, the autumn and winter phenophases, including sowing, germination and dormancy, are mainly delayed, while spring and summer phenophases, including re-gree~~n~~ning and maturity, are primarily advanced. According to the fitting coefficient (a), the duration ~~were~~ was changed by 5.7, 8.1, 4.9, -3.5, and -5.5 in the period of 1981-2009, respectively, for the stages of sowing, germination, dormancy, re-gree~~n~~ning and maturity of winter wheat. These results were consistent with our previous studies (Tao et al. 2012; Xiao et al. 2013; Xiao et al. 2015)~~, and indicating that the selected stations were good representation of the NCP~~.

Table 3 General information on the phenology of winter wheat in the selected stations (unit: DOY)

Station	Period	Sowing	Germination	Dormancy	Re-greening	Maturity
Miyun	1981-2009	275.52±7.55	284.96±9.03	331.93±6.41	73.59±15.1	168.26±3.46
Baodi	1981-2009	272.83±4.33	281.55±5.5	335.62±6.86	59.19±42.72	165.97±2.57
Tangshan	1981-2009 (except 2003)	271.86±4.83	279.59±6.04	335.55±6.6	66.62±7.98	169.97±3.23
Huanghua	1981-2009	274.17±7.83	280.32±7.03	340.38±8.65	62.45±6.56	157.14±3.25
Weifang	1981-2009	274.1±5.75	284.62±17.93	343.72±7.76	59.59±7.29	160.41±3.42
Xinxiang	1981-2009	283.59±4.21	291.64±5.14	351.9±10.56	47.55±7.16	152.03±3.3
Zhengzhou	1981-2009	289.76±5.67	298.45±6.65	360.5±14.08	44.21±7.43	151.34±3.88

带格式的: 字体: (默认) Times New Roman

Shangqiu	1981-2009	287.59±4.07	295.31±4.79	359.21±32.4	47.03±6.43	151.59±2.99
Nanyang	1981-2009	297.21±7.81	306.83±9.03	7.54±14.64	48.22±8.9	149.21±4.99
Zhumadian	1981-2009 (except 1986, 1988)	289.54±9.33	298.29±11.11	5.46±10.35	49.15±6.84	146.21±4.76

the data was shown in average ± standard deviation.

Table 4 Linear trends in winter wheat phenology

Station	Sowing		Germination		Dormancy		Re-greening		Maturity	
	a	p	a	p	a	p	a	p	a	p
Miyun	**0.62**	**0.00**	**0.69**	**0.00**	0.17	0.27	-0.51	0.15	**-0.20**	**0.01**
Baodi	**0.31**	**0.00**	**0.41**	**0.00**	0.14	0.36	-0.67	0.52	-0.05	0.35
Tangshan	**0.41**	**0.00**	**0.51**	**0.00**	**0.43**	**0.00**	-0.29	0.11	**-0.20**	**0.00**
Huanghua	0.18	0.31	0.17	0.31	0.38	0.05	-0.07	0.64	-0.13	0.07
Weifang	0.20	0.11	0.61	0.13	0.11	0.55	0.14	0.38	-0.12	0.11
Xinxiang	0.07	0.46	0.12	0.34	0.27	0.26	-0.16	0.33	-0.12	0.10
Zhengzhou	-0.16	0.21	-0.21	0.17	-0.28	0.41	0.11	0.52	**-0.25**	**0.00**
Shangqiu	0.03	0.77	0.04	0.68	0.39	0.59	0.10	0.51	-0.07	0.28
Nanyang	-0.18	0.30	-0.11	0.60	-0.13	0.71	0.12	0.60	**-0.38**	**0.00**
Zhumadian	**0.49**	**0.02**	**0.56**	**0.02**	0.21	0.37	0.02	0.89	**-0.36**	**0.00**

a was the coefficient of linear fitting equation (d/year); p was the significance level;

bolded number means $p < 0.05$.

2.3 Methods

2.3.1 Model calibration and verification

带格式的：字体：加粗

The SiBcrop model was selected in this study. SiBcrop is a process-based land surface model adapted from the Simple Biosphere model version 3 (Lokupitiya et al. 2009). The SiB series models (version 1, 2, 3 refers to SiB1, SiB2, SiB3, respectively) are widely adopted land surface models for computing surface energy, water, momentum and CO_2 exchange in the boundary layer. The SiBcrop version added the crop-specific submodels~~simulation~~ of maize, soybean, winter and spring wheats, which ~~cropping system (Lokupitiya et al. 2009). The crop-specific submodel~~ was simple and detailed enough in predicting LAI (Lokupitiya et al. 2009). ~~replaces remotely-sensed NDVI information by simulated LAI and the fraction of photosynthetically active radiation.~~ The submodel replaces remotely-sensed NDVI information by simulated LAI. SiBcrop simulated fast response processes that vary sub-hourly such as energy, water, carbon and momentum balance of the canopy and soil, as well as the processes that vary daily such as LAI. Surface energy and water fluxes are calculated at each time step on a grid cell basis according to physiologically based formulations of leaf-level photosynthesis, stomatal conductance and respiration (Farquhar et al. 1980; Collatz et al. 1990).

The model was first modified according to the actual situation of winter wheat in the NCP (Chen et al. 2020). The SiBcrop model was originally calibrated in winter wheat – summer fallow system in which the growth time of wheat is relatively abundant (Lokupitiya et al. 2009). However, the NCP is dominated by winter wheat – summer maize system in which the development of wheat is strictly restricted. There are great differences in the varieties, planting date, growth environment and physiological characteristics of winter wheat between the two systems. The modifications ~~including~~include: (1) the sowing date was postponed to October from original August. (2)

带格式的：字体：小四

带格式的：字体：小四

带格式的：字体：小四

带格式的：字体：小四

tolerance was reduced to 8℃ from original 18℃, above which the seven consecutive days for wheat sowing ~~was~~ were counted. (3) The harsh condition of delayed sowing also the daily growth rate, which was modified from 0.07 to 0.03 g m^{-2} when GDD was 105-310 ºC d. (4) Wheat grows faster when GDD is 769-1074 ºC d with maximum dry weight increased from 8 to 12 g and daily rate enlarged from 0.015 to 0.15 g m^{-2}. (5) Specific leaf area was changed from 0.02 to 0.025 m^2 g^{-1} (Najeeb et al. 2016). (6) A subroutine was added to describe the senescence process of canopy when GDD was larger than 1074 ºC d according to Tao et al~~.~~ (Tao et al. 2009). More details could be referred to Chen et al (2020).

After modifications, the simulated biases were within 10 days for wheat emergency and harvest dates, the determination coefficient, root mean square error, and agreement index between simulated and observed LAI were obviously improved from 0.26, 1.89 m^2 m^{-2}, and 0.7 to 0.80, 0.99 m^2 m^{-2}, and 0.91, respectively. And they were 0.66, 32.37 W m^{-2}, and 0.84, respectively, for the simulated *LH* (Chen et al. 2020).

2.3.2 Model simulation

Two simulations with different sowing dates were performed to examine the responses of surface biophysical processes~~ to shifts in sowing dates~~ at the selected 10 stations (Fig.1). The planting date was classified into two scenarios: after DOY 265 (early sowing scenario, EP) and after DOY 275 (late sowing scenario, LP). The early and late sowing scenarios were established by artificially limiting the starting time of the sowing date.~~–~~ The early sowing scenario means that the sowing will not be allowed until DOY 265. Similarly, the late sowing scenario is only allowed after DOY 275. In both scenarios, wheat was sowed at the seventh consecutive days when temperature ranged ~~5~~8~~~~25℃,

which means the real sowing date was seven days later. The SiBcrop model was modified to be more cold tolerance (section 2.3.1), which causing the sowing date was less controlled by temperature. The climate variability among stations has less constraint on sowing date. Our previous study showed that the delayed sowing date of winter wheat was mainly caused by the delayed harvest of maize in the NCP (Xiao et al. 2013). The sowing date in the two scenarios is within the climatological average of the region.

2.3.3. Methods to relate the surface energy balance components with T_c

The Boisier method (Boisier et al. 2012) was adopted to relate the surface energy balance components with T_c. The energy partitioning of a terrestrial surface is expressed as

$$(1-\alpha)\, S_d + L_d - L_u = LH + SH + R \qquad (1)$$

Where S_d, L_d, and L_u are the downward short-wave radiation, downward long-wave radiation, and upward long-wave radiation, respectively. In order to have a closed surface energy balance, the residual term R was derived explicitly from the other terms in equation (1), and principally accounts for the soil heat flux and canopy storage flux.

The T_c change simulated by model is affected by both radiative (surface albedo effect) and non-radiative processes (surface energy partitioning effect). In order to separate temperature variation caused by the sole change in absorbed short-wave radiation (radiative process), the following equation (Boisier et al. 2012) was used:

$$\Delta T_c = (\varepsilon\sigma)^{-1/4}\left[\left(L_u + \Delta L_u\right)^{1/4} - L_u^{1/4}\right] \qquad (2)$$

Where ΔT_c is the anomaly of canopy temperature (K). The σ is Stefan-Boltzmann constant (=5.67×10 -8 W m^{-2} K^{-4}). The ε is surface emissivity (= 1). A disturbance in S_d,

299 L_d, *LH*, *SH* or *R* can be expressed as ΔL_u by fixing non-perturbed terms using equation
300 (1). More details can be found in Boisier et al. (2012).
301
302 **3 Results**
303 **3.1 SiBcrop simulation accuracy**
304 ~~The SiBcrop model had been modified to improve the simulation accuracy of wheat~~
305 ~~growth and surface fluxes in our previous study (Chen et al. 2020). After modifications,~~
306 ~~the simulated biases were within 10 days for wheat emergency and harvest dates, the~~
307 ~~determination coefficient, root mean square error, and agreement index between~~
308 ~~simulated and observed LAI were obviously improved from 0.26, 1.89 $m^2 m^{-2}$, and 0.7 to~~
309 ~~0.80, 0.99 $m^2 m^{-2}$, and 0.91, respectively. And they were 0.66, 32.37 W m^{-2}, and 0.84,~~
310 ~~respectively, for the simulated *LH* (Chen et al. 2020).~~
311 The simulation error for wheat phenology at Yucheng station was within 10 days
312 (Chen et al. 2020). The sowing time under the two sowing scenarios was further
313 compared with observation at the selected 10 stations. The simulated sowing date was
314 stable, generally around DOY278.66 ± 1.15, and DOY 290.34 ± 2.08 for EP and LP
315 scenario, respectively. The observed phenology fluctuated greatly. Wheat was prone to
316 sow later or early generally due to geographical location at some specific stations. In the
317 EP scenario, the stations in the north had a positive difference (delayed sowing date
318 relative to the actual date) compared to the actual phenological period, whereas the
319 stations in the south had a negative difference (advanced sowing date relative to the
320 actual date), because the stations in the north had earlier sowing date than those in the
321 south. In the LP scenario, the stations in the south were relatively close to the actual

phenology, but the stations near the north had a larger positive difference. Overall, the simulation difference of phenology was within 15 days. ~~The selected scenario covers the actual situation of winter wheat sowing in the NCP. The comparisons improved the representativeness and reliability of the simulation results.~~

Table 5 The difference between simulated and observed sowing dates under two scenarios at each station

Station	Scenario	
	Early sowing	Late sowing
Miyun	4.19±7.82	17.48±7.55
Baodi	6.59±4.62	19.59±4.49
Tangshan	7.41±4.95	20.38±5.47
Huanghua	4.41±8.02	16.31±7.55
Weifang	4.34±5.6	15.86±5.55
Xinxiang	-5.31±4.24	5.59±4.24
Zhengzhou	-11.41±5.47	-0.38±5.53
Shangqiu	-9.34±3.84	1.48±3.85
Nanyang	-19.07±7.87	-8.41±8.08
Zhumadian	-11.36±8.91	-0.57±9.07
All	-2.98±10.96	8.7±11.66

data was show in average ± standard deviation.

3.2 Seasonal dynamics of LAI and T_c in scenarios

Wheat LAI curves for the two sowing dates were ~~obviously~~ not overlapped (Fig.2a). The LAI in the EP scenario was larger with earlier development. With the sowing in the LP scenario, LAI difference between the two scenarios gradually narrowed until the spring of the next year when the disparity increased again (Fig.3a). The LAI difference between two scenarios had a valley after the reproductive period. With the approaching of harvest, the difference gradually decreased to 0.

The LAI difference of winter wheat in two scenarios is mainly attributed to the difference in the accumulation of ~~organic matter~~biomass. In the EP scenario, earlier sowing means advanced assimilation process and better temperature conditions, more photosynthetic carbon was produced and distributed into leaf. The impact of sowing time on LAI displayed great dissimilarity among stations (Fig.3a). Based on linear regression, the seasonal average of wheat LAI difference between scenarios was highly related with precipitation in the growth period (LAI anomaly = 0.0011 * P - 0.12，R^2 = 0.59). The more precipitation, the greater influence of sowing date on growth. The T_a contributed little to the LAI difference between the two scenarios.

According to the T_c difference between scenarios, the following phenologies of winter wheat were relatively important: sowing date, dormancy date, re-greening date and maturity date. Based on the simulation results, the phenological dates used here as follows: EP sowing date, DOY279; LP sowing date, DOY290; dormancy date, DOY334; re-greening date, DOY59; maturity date, DOY170 (Fig.2a). The T_c difference between scenarios was separated into 4 phases: Phase 1, inter-sowing period, when wheat had been sown in the EP but hadn’t in the LP; Phase 2: early growing period, from sowing

带格式的: 字体: (默认) Times New Roman, 小四, 字体颜色: 自动设置, 图案: 清除
带格式的: 字体: (默认) Times New Roman, 小四, 字体颜色: 自动设置, 图案: 清除
带格式的: 缩进: 首行缩进: 2 字符
带格式的: 字体: (默认) Times New Roman, 小四, 字体颜色: 自动设置, 图案: 清除
带格式的: 字体: (默认) Times New Roman, 小四, 字体颜色: 自动设置, 图案: 清除
带格式的: 字体: (默认) Times New Roman, 小四, 字体颜色: 自动设置, 图案: 清除
带格式的: 字体: (默认) Times New Roman, 小四, 字体颜色: 自动设置, 图案: 清除
带格式的: 字体: (默认) Times New Roman, 小四, 字体颜色: 自动设置, 图案: 清除
带格式的: 字体: (默认) Times New Roman, 小四, 字体颜色: 自动设置, 图案: 清除
带格式的: 字体: (默认) Times New Roman, 小四, 字体颜色: 自动设置, 图案: 清除
带格式的: 字体: (默认) Times New Roman, 小四, 字体颜色: 自动设置, 图案: 清除
带格式的: 字体: (默认) Times New Roman, 小四, 字体颜色: 自动设置, 图案: 清除
带格式的: 字体: (默认) Times New Roman, 小四, 字体颜色: 自动设置, 图案: 清除
带格式的: 字体: (默认) Times New Roman, 小四, 字体颜色: 自动设置, 图案: 清除
带格式的: 无下划线

date of LP to dormancy date; Phase 3: dormancy period, from dormancy date to re-greening date; Phased 4: late growing period, from re-greening date to maturity date (Fig.2b).

The most obvious disparity in T_c between two scenarios occurred in the inter-sowing period when wheat had been sown in the EP but hadn’t in the LP (Fig.2b). The development of early sown winter wheat resulted in higher T_c, with a peak of up to 0.6 K. The growth of wheat in the LP sharply reduced the warming effect in EP, and eventually the EP scenario had lower temperatures (-0.2K) before entering the dormancy period. The temperature change process during this period was relatively consistent across the selected stations (Fig.3b). In the late growing period, the EP had lower temperature (-0.1 K) than LP. In particular, LAI difference varied greatly between statioms (Fig.3a), T_c difference was relatively stable (Fig.3b).

Another special period is the dormancy period, when EP had higher T_c than LP with an average of 0.05 K (Fig.3b). With the start of the re-greening period, the EP T_c was gradually lower than LP T_c and dropped to 0 at the harvest time. The T_c dynamics during this period was highly heterogeneous among the stations, varying between -0.25~0.25 K.

In the dormancy period, the T_c anomaly between scenarios was significantly affected by the T_a in winter (T_c anomaly = -0.023 * T_a + 0.062, R^2 = 0.6, p = 0.005). The lower the T_a, the bigger the T_c difference, which indicating that the influence of sowing date is more important in northern farmland. The linear relationship between P and T_c difference in winter was not obvious. The linear fitting equation between P and T_c anomaly in the growing period: T_c anomaly = -0.0013 * P + 0.057, R^2 = 0.8, p < 0.001. So mMore rainfall increased the T_c anomaly in the growing period. The linear fitting equation

带格式的: 字体: (默认) Times New Roman, 小四, 字体颜色: 自动设置, 图案: 清除

带格式的: 字体: (默认) Times New Roman, 小四, 字体颜色: 自动设置, 图案: 清除

带格式的: 字体: (默认) Times New Roman, 小四, 字体颜色: 自动设置, 图案: 清除

带格式的: 字体: (默认) Times New Roman, 小四, 字体颜色: 自动设置, 图案: 清除

带格式的: 字体: (默认) Times New Roman, 小四, 字体颜色: 自动设置, 图案: 清除

带格式的: 字体: (默认) Times New Roman, 小四, 字体颜色: 自动设置, 图案: 清除

带格式的: 字体: (默认) Times New Roman, 小四, 字体颜色: 自动设置, 图案: 清除

between T_a and T_c anomaly in the growing period: T_c anomaly = -0.017 * T_a + 0.2, R^2 = 0.53, p = 0.01. Since the T_c anomaly was negative, the higher the T_a, the greater the T_c anomaly. Considering the low temperature and less precipitation at the northern stations, the high temperature and more precipitation at the southern stations, the climate feedback of sowing date ~~shift~~ was more obvious in winter in the northern areas, and in the growing period in the southern areas.

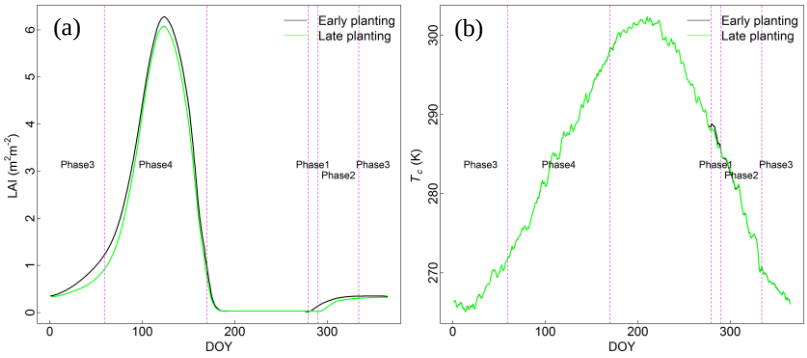

Fig.2 Dynamics of (a) LAI and (b) T_c under two sowing scenarios in winter wheat growing season

Phase 1: inter-sowing period, when wheat had been sown in the EP but hadn't in the LP; Phase 2: early growing period, from sowing date of LP to dormancy date; Phase 3: dormancy period, from dormancy date to re-greening date; Phased 4: late growing period, from re-greening date to maturity date.

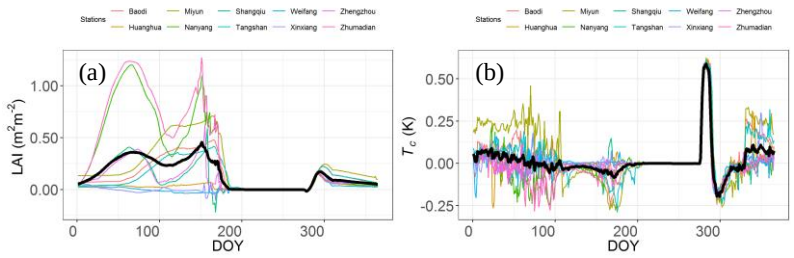

Fig.3 Seasonal differences in (a) LAI and (b) T_c of EP-LP at each station. The average across the stations was shown in bold black line

3.3 Contributions of surface energy balance components to scenario difference in T_c

According to the seasonal dynamics of LAI and T_c, winter wheat growth could not explain the difference in climate effect of sowing time. Specifically, the T_c anomaly between the two scenarios ~~were~~ was reversed between the dormancy (Phase 3~~December, January, and February~~) and active growth periods (Phase 2 and Phase 4~~other wheat development period with active physiological activity~~), but with both positive LAI difference (Fig.3). In this section, surface energy balance was used to explain the response of T_c to sowing date.

The flux anomalies of R_n, *LH*, *SH* and *R* were shown in Fig.4a. The EP scenario always maintained higher R_n and *LH*. Especially winter wheat-covered ground captured more than 10 W m^{-2} R_n than bare land. The anomaly of R_n in different sowing dates was maintained within 2 W m^{-2}. *LH* generally was covariant with the change in R_n. However, the anomaly of *LH* in the late growth period was greater than that of R_n, resulting in negative *SH*, indicating that the EP scenario had stronger *LH* distribution tendency and

less *SH* was partitioned. Bigger anomaly of *SH* was happened in the initial and dormant stages. *R* anomaly fluctuated obviously only in the initial phase.

The contributions of surface energy balance components to T_c were shown in Fig.4b. Stronger radiation absorption provided more energy for the thermal motion of air and causing positive T_c differences of EP-LP. Correspondingly, higher distribution into *LH*, *SH*, and *R* was conducive to cooling T_c. Therefore, positive *LH* and *SH* differences of EP-LP showed negative T_c effects, and negative *R* difference of EP-LP showed positive T_c effect. The positive T_c anomaly of EP-LP reflected that the radiative process played the major role in the dormancy period. In the active growth time, the cooling effect of *LH* partitioning dominated the T_c anomaly.

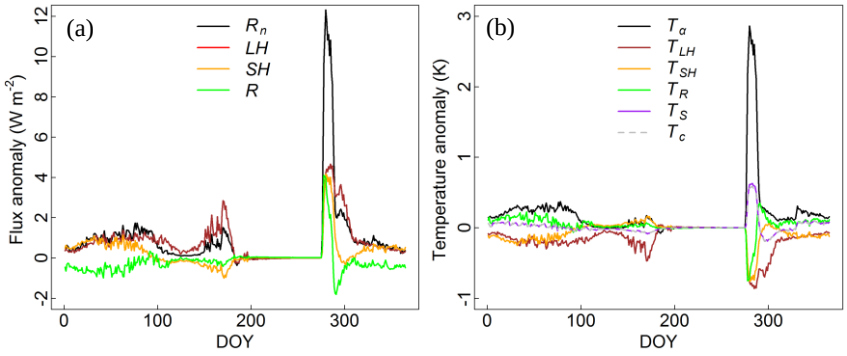

Fig.4 (a) The differences in the surface fluxes between the sowing scenarios of EP and LP, (b) its contributions to T_c anomaly.

R_n means net radiation, T_a represents the temperature anomaly induced by changes in absorbed solar radiation. T_{LH} represents the temperature anomaly induced by changes in latent flux. T_{SH} represents the temperature anomaly induced by changes in sensible flux. T_R represents the temperature anomaly induced by changes in residual term. T_S represents

the temperature anomaly induced by changes in solar radiation, latent, sensible and residual fluxes.

4 Discussion

4.1 The diverse ~~shift~~ trends in sowing date of winter wheat in the NCP

The spatiotemporal changes of winter wheat phenology had been ~~examined~~extensively examined in ~~,~~ the NCP. In the period of 1981-2009, the sowing date was on average delayed by 1.5 days/decade, but ~~In the period of 1981-2009, sowing date delayed significantly at 13 station and advanced at~~ 8 ~~stations~~ out of the 36 agro-meteorological experiment stations were advanced (Xiao et al. 2013). ~~In the NCP, the sowing date were on average delayed by 1.5 day/decade.~~ The diverse trends in sowing date were also existed at the national scale, where 6 stations significantly advanced by up to 9.1 days/decade, and 11 stations significantly delayed by up to 10 days/decade (Tao et al. 2012).

The proper sowing date is key to ensure winter wheat survive~~d~~ through winter and reduce the freezing injury, insect pests and other harmful conditions (Sacks et al. 2010; Zhang et al. 2012; Newbery et al. 2016). With faster growth in warmer environment, the sowing date should be postponed to maintain ~~the~~ a proper coverage of winter wheat in dormancy period. The warming of the NCP is regionally consistent (Shi et al. 2014), and the diverse change of sowing date will affect the coverage of winter wheat, especially one fifth stations advanced their sowing date. Earlier sowing may also benefited from the reduction in freezing damage and the increase in pest diseases caused by higher minimum

带格式的：两端对齐

temperature, since more above-ground biomass will not be subject to lethal freezing damage and will resist higher harms from pests and diseases. There are also management practices to counteract the effects of advanced sowing date, such as deep tillage and delayed irrigation, which reduce the development of leaves and stems. Until now, fewer studies had focused on the phenomenon of early sowing date and its underlying causes and countermeasures.

带格式的: 字体: (默认) Times New Roman, 小四, 字体颜色: 自动设置, 图案: 清除

Although there were literatures reporting that the albedo process in winter is relatively important (Richardson et al. 2013; Lombardozzi et al. 2018), fewer studies directly addressed the influence of different surface characteristics and climate effect through biophysical process in the dormancy period. In the Oklahoma's winter wheat belt, the rapid crop growth during November exhibited a distinct cool anomaly against adjacent regions of dormant grassland. Over the period of December through April, the cool bias was visibly diminished although the greenness difference between grassland and wheat was more distinct (McPherson et al. 2004). The biophysical impacts between maize and perennial grass were simulated using Agro-IBIS model in US corn belt (Bagley et al. 2015). The results showed that much higher LAI of perennial scenario was existed in winter December–February (3 vs 0 m^2 m^{-2}) and in summer June–August (10 vs 4 m^2 m^{-2}). Perennial grass had smaller surface albedo (coupling snow effect) than maize in winter, but showed quite small difference in summer. During winter and summer, the perennial scenario had slightly higher *LH* than the maize scenario, but the difference in R_n between two scenarios was more than 10W m^{-2} in winter (Bagley et al. 2015). The above

studies indicated that the cooling effect of higher LAI was inhibited in winter. The results of this current study indicate that higher LAI in winter has a warming effect~~, which is different from the conclusion above~~. The main reason was due to the relative contributions of surface albedo mechanism and surface flux distribution process.

The strong climate feedback in inter-sowing period, when wheat had been sown in the EP but hadn't in the LP, was related to the effect of tillage on maize stubble. The NCP is dominated by summer maize - winter wheat rotation system in which the ground is covered with maize stubble before wheat is sown. The damage of sowing to stubble is conducive to the reduction of albedo since stubble has larger surface reflectivity than soil (O'Brien et al. 2019). The 0.1 increase of surface albedo caused by no-till management, which was also the magnitude of our simulation (Table 6), cooling the hottest summer days by 2 °C or more (Davin et al. 2014). The inter-sowing period is equivalent to no-tillage period, when early sowed wheat absorbed more net radiation with lower albedo by destroying stubble and causing higher temperature (Fig.3b, Fig4a).

Previous studies showed that the increase of vegetation cover caused warming feedback by destroying the high albedo of snow in the case of snow cover (Richardson et al. 2013; Bagley et al. 2015; Lombardozzi et al. 2018). In our simulation, except for the large difference in crop coverage in phase 1, the snow and crop had consistent coverage in other phases (Supplement Table 1), which means albedo difference between two scenarios was not caused by snow. Low soil water content ~~also~~ contributed to the high surface albedo (Seneviratne et al. 2010)(Fig.6b). With the decrease of surface soil moisture, surface albedo increased in winter, which explained why albedo in the winter

带格式的: 字体: (默认) Times New Roman, 小四

带格式的: 字体: (默认) Times New Roman, 小四

带格式的: 字体: (默认) Times New Roman, 小四, 字体颜色: 自动设置, 图案: 清除

带格式的: 字体: (默认) Times New Roman, 小四, 字体颜色: 自动设置, 图案: 清除

带格式的: 字体: (默认) Times New Roman, 小四, 字体颜色: 自动设置, 图案: 清除

带格式的: 字体: (默认) Times New Roman, 小四, 字体颜色: 自动设置, 图案: 清除

was higher than that in the growth period. The increase in soil reflectivity caused by soil drying enhanced the role of low winter wheat reflectivity in surface albedo, the albedo disparity between the two scenarios increased in winter, ~~so~~ which strengthened the albedo-radiative mechanism ~~strengthened~~. Low soil moisture also contributed to the disparity in warming effect between EP and LP during dormancy period (Fig.6b). The lack of precipitation in winter made soil moisture unable to be replenished effectively, thus reducing soil evaporation and crop transpiration. But during the growing season, soil moisture is high enough to supply transpiration. The lower the T_a, the lower the transpiration vitality, thus unable to offset the warming effect of increased R_n absorption, which explained why the winter T_c disparity among stations was controlled by T_a.

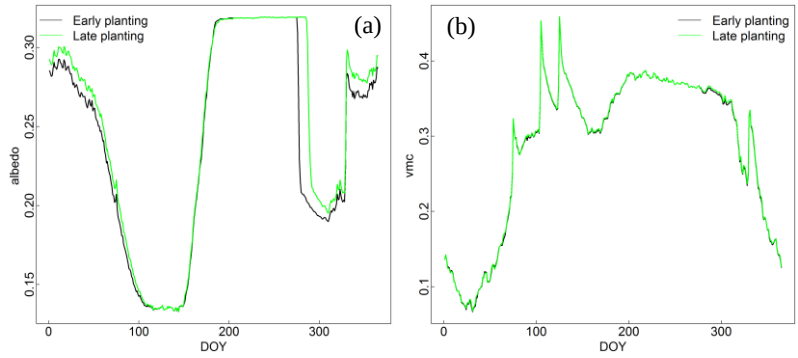

Fig.6 Dynamics of (a) surface albedo and (b) surface soil moisture content under two sowing scenarios in winter wheat growing season

Table 6 The reflectivity of different surface coverings in near-infrared and visible bands in the SiBcrop model

Material	Visible band	Near Infrared band
Green leaf	0.08	0.3

Snow	0.8	0.4
Soil with crop	0.11	0.314
Bare soil	0.33	0.35

4.3 Cooling effect of EP-LP during the growing period

The phenological shifts, such as earlier leaf unfolding, delayed leaf fall, and lengthening of the green-cover season have feedback on climate through biophysical and biogeochemical processes (Penuelas et al. 2009). Previous studies showed cooling effect in the photosynthetic active period through surface biophysical mechanism in the cropland (e.g. (Sacks and Kucharik 2011; Zhang et al. 2013; Bohm et al. 2020)).

In the NCP, the increased spring surface greenness at farmland, benefited from advanced re-greening stage of winter wheat (Xiao et al. 2013; Liu et al. 2017), had cooling and wetting effects (Zhang et al. 2013) and suppressed the moderate to light rainfall (Zhang et al. 2015). The analysis found that surface greening increased the partitioning into *LH* and reduced *SH* to cooling surface air and suppression of rainfall (Zhang et al. 2013; Zhang et al. 2015). Distinguished difference between early-covering crops (winter wheat, winter rapeseed, winter barley) and late-covering crops (corn, silage maize, sugar beet) in central Europe caused impacts on simulated surface energy fluxes and temperature in the Noah-MP model, the higher LAI led to an increase in *LH*, decreased in *SH* and eventually surface cooling in May-September (Bohm et al. 2020). The Agro-IBIS model was used to study the impacts on surface energy balance of advanced corn sowing date (10 days): Early sowing means earlier development and

带格式的: 缩进：首行缩进： 1.5 字符

senescence of LAI, causing stronger disparity of LH than R_n with bigger LAI and probably a slight cooling of T_a in June (Sacks and Kucharik 2011). Similar conclusions were presented based on simulated T_c results with modified SiBcrop.

5 Conclusions

The dynamics of winter wheat LAI and T_c under two sowing date scenarios were simulated by the SiBcrop model in the NCP, and the T_c disparity between the two scenarios was explained by the surface energy balance. The findings include:

(1) Earlier sowing date of winter wheat had higher LAI than later sowing date.

(2) The T_c disparity between EP and LP is divided into two periods: warming effect in the dormancy period, and cooling effect in the active growth period.

(3) Surface energy balance can interpret the climate feedback mechanism of sowing date ~~shift~~, that is, the dominated role of albedo-radiative process in the dormancy period is surpassed by LH partitioning-non-radiative process in the growth period.

(4) The responses of LAI and T_c to sowing date at station scale were divergent: controlled by T_a in the dormancy period, and influenced by P and T_a in the growth period.

The study had some shortcomings. The single model simulation was highly dependent on the structure and parameterization scheme of the model. The climate feedback was reflected by the canopy temperature. In the SiBcrop model, the spatial distribution of stations was not fully considered in the determination of sowing date, which resulted in too early or too late sowing at some stations.

~~showed that even when land use/cover type remains unchanged, variations in surface~~

Acknowledgments

This study is supported by the National Natural Science Foundation of China (41801020).

References

A, D., Xiong, K., Zhao, W., Gong, Z., Jing, R., and Zhang, L.: Temporal trend of climate change and mutation analysis of North China Plain during 1960 to 2013. Scientia Geographica Sinica, 36(10), 1555-1564, 2016.

Bagley, J. E., Kueppers, L. M., Billesbach, D. P., Williams, I. N., Biraud, S. C., and Torn, M. S.: The influence of land cover on surface energy partitioning and evaporative fraction regimes in the US Southern Great Plains. Journal of Geophysical Research-Atmospheres, 122(11), 5793-5807, 2017.

Bagley, J. E., Miller, J., and Bernacchi, C. J.: Biophysical impacts of climate‐smart agriculture in the Midwest United States. Plant, cell & environment, 38(9), 1913-1930, 2015.

Bohm, K., Ingwersen, J., Milovac, J., and Streck, T.: Distinguishing between early- and late-covering crops in the land surface model Noah-MP: impact on simulated surface energy fluxes and temperature. Biogeosciences, 17(10), 2791-2805, 2020.

Boisier, J. P., de Noblet-Ducoudre, N., Pitman, A. J., Cruz, F. T., Delire, C., van den Hurk, B. J. J. M., et al.: Attributing the impacts of land-cover changes in temperate regions on surface temperature and heat fluxes to specific causes: Results from the first LUCID set of simulations. Journal of Geophysical Research-Atmospheres, 117, 2012.

Chen, M., Griffis, T. J., Baker, J., Wood, J. D., and Xiao, K.: Simulating crop phenology in the Community Land Model and its impact on energy and carbon fluxes. Journal of Geophysical Research-Biogeosciences, 120(2), 310-325, 2015.

Chen, Y., Liu, F., Tao, F., Ge, Q., Jiang, M., Wang, M., et al.: Calibration and validation of SiBcrop Model for simulating LAI and surface heat fluxes of winter wheat in the North China Plain. Journal of Integrative Agriculture, 19(9), 2-11, 2020.

Cho, M. H., Boo, K. O., Lee, J., Cho, C., and Lim, G. H.: Regional climate response to land surface changes after harvest in the North China Plain under present and possible future climate conditions. Journal of Geophysical Research-Atmospheres, 119(8), 4507-4520, 2014.

Collatz, G. J., Berry, J. A., Farquhar, G. D., and Pierce, J.: The relationship between the Rubisco reaction mechanism and models of photosynthesis*. Plant, Cell & Environment, 13(3), 219-225, 1990.

Cooley, H. S., Riley, W. J., Torn, M. S., and He, Y.: Impact of agricultural practice on regional climate in a coupled land surface mesoscale model. Journal of Geophysical Research Atmospheres, 110(D03113, doi:10.1029/2004JD005160.), -, 2005.

Cui, J., Yan, P., Wang, X., Yang, J., Li, Z., Yang, X., et al.: Integrated assessment of economic and environmental consequences of shifting cropping system from wheat-maize to monocropped maize in the North China Plain. Journal of Cleaner Production, 193, 524-532, 2018.
Davin, E. L., Seneviratne, S. I., Ciais, P., Olioso, A., and Wang, T.: Preferential cooling of hot extremes from cropland albedo management. Proceedings of the National Academy of Sciences of the United States of America, 111(27), 9757-9761, 2014.
Eyshi Rezaei, E., Siebert, S., and Ewert, F.: Climate and management interaction cause diverse crop phenology trends. Agricultural and Forest Meteorology, 233, 55-70, 2017.
Falge, E., Baldocchi, D., Olson, R., Anthoni, P., Aubinet, M., Bernhofer, C., et al.: Gap filling strategies for defensible annual sums of net ecosystem exchange. Agricultural and Forest Meteorology, 107(1), 43-69, 2001.
Farquhar, G. D., von Caemmerer, S., and Berry, J. A.: A biochemical model of photosynthetic CO2 assimilation in leaves of C3 species. Planta, 149(1), 78-90, 1980.
Goudriaan, J. 1977. Crop micrometeorology : a simulation study, Pudoc.
Hammerle, A., Haslwanter, A., Tappeiner, U., Cernusca, A., and Wohlfahrt, G.: Leaf area controls on energy partitioning of a temperate mountain grassland. Biogeosciences, 5(2), 421-431, 2008.
Ho, C.-H., Park, S.-J., Jeong, S.-J., Kim, J., and Jhun, J.-G.: Observational Evidences of Double Cropping Impacts on the Climate in the Northern China Plains. Journal of Climate, 25(13), 4721-4728, 2012.
Jeong, S.-J., Ho, C.-H., Piao, S., Kim, J., Ciais, P., Lee, Y.-B., et al.: Effects of double cropping on summer climate of the North China Plain and neighbouring regions. Nature Clim. Change, 4(7), 615-619, 2014.
Lei, H., Yang, D., Lokupitiya, E., and Shen, Y.: Coupling land surface and crop growth models for predicting evapotranspiration and carbon exchange in wheat-maize rotation croplands. Biogeosciences, 7(10), 3363-3375, 2010.
Liu, C., Gao, Z., Li, Y., Gao, C. Y., Su, Z., and Zhang, X.: Surface Energy Budget Observed for Winter Wheat in the North China Plain During a Fog–Haze Event. Boundary-Layer Meteorology, 170(3), 489-505, 2019.
Liu, F., Chen, Y., Shi, W., Zhang, S., Tao, F., and Ge, Q.: Influences of agricultural phenology dynamic on land surface biophysical process and climate feedback. Journal of Geographical Sciences, 27(9), 1085-1099, 2017.
Liu, J., Liu, M., Tian, H., Zhuang, D., Zhang, Z., Zhang, W., et al.: Spatial and temporal patterns of China's cropland during 1990–2000: An analysis based on Landsat TM data. Remote Sensing of Environment, 98(4), 442-456, 2005.
Liu, S., Xu, Z., Zhu, Z., Jia, Z., and Zhu, M.: Measurements of evapotranspiration from eddy-covariance systems and large aperture scintillometers in the Hai River Basin, China. Journal of Hydrology, 487, 24-38, 2013.
Liu, S. M., Xu, Z. W., Wang, W. Z., Jia, Z. Z., Zhu, M. J., Bai, J., et al.: A comparison of eddy-covariance and large aperture scintillometer measurements with respect to the energy balance closure problem. Hydrology and Earth System Sciences (HESS) & Discussions (HESSD), 15, 1291-1306, 2011.
Liu, Y. A., Wang, E. L., Yang, X. G., and Wang, J.: Contributions of climatic and crop varietal changes to crop production in the North China Plain, since 1980s. Global Change Biology, 16(8), 2287-2299, 2010.

637 Liu, Y. J., Chen, Q. M., Ge, Q. S., Dai, J. H., Qin, Y., Dai, L., et al.: Modelling the
638 impacts of climate change and crop management on phenological trends of spring and
639 winter wheat in China. Agricultural and Forest Meteorology, 248, 518-526, 2018.
640 Liu, Z., Wu, C., Liu, Y., Wang, X., Fang, B., Yuan, W., et al.: Spring green-up date
641 derived from GIMMS3g and SPOT-VGT NDVI of winter wheat cropland in the North
642 China Plain. Isprs Journal of Photogrammetry & Remote Sensing, 130, 81-91, 2017.
643 Lokupitiya, E., Denning, S., Paustian, K., Baker, I., Schaefer, K., Verma, S., et al.:
644 Incorporation of crop phenology in Simple Biosphere Model (SiBcrop) to improve
645 land-atmosphere carbon exchanges from croplands. Biogeosciences, 6(6), 969-986, 2009.
646 Lombardozzi, D. L., Bonan, G. B., Wieder, W., Grandy, A. S., Morris, C., and Lawrence,
647 D. M.: Cover Crops May Cause Winter Warming in Snow‐Covered Regions.
648 geophysical research letters, 45(18), 9889-9897, 2018.
649 Mahdi, L., Bell, C. J., and Ryan, J.: Establishment and yield of wheat (Triticum turgidum
650 L.) after early sowing at various depths in a semi-arid Mediterranean environment. Field
651 Crops Research, 58(3), 187-196, 1998.
652 Mahmood, R., Pielke, R. A., Hubbard, K. G., Niyogi, D., Dirmeyer, P. A., McAlpine, C.,
653 et al.: Land cover changes and their biogeophysical effects on climate. International
654 Journal of Climatology, 34(4), 929-953, 2014.
655 McPherson, R. A., Stensrud, D. J., and Crawford, K. C.: The Impact of Oklahoma's
656 Winter Wheat Belt on the Mesoscale Environment. Monthly Weather Review, 132(2),
657 405-421, 2004.
658 Mirschel, W., Wenkel, K.-O., Schultz, A., Pommerening, J., and Verch, G.: Dynamic
659 phenological model for winter rye and winter barley. European Journal of Agronomy,
660 23(2), 123-135, 2005.
661 Najeeb, U., Bange, M. P., Atwell, B. J., and Tan, D. K. Y.: Low Incident Light Combined
662 with Partial Waterlogging Impairs Photosynthesis and Imposes a Yield Penalty in Cotton.
663 Journal of Agronomy and Crop Science, 202(4), 331-341, 2016.
664 Newbery, F., Qi, A., and Fitt, B. D.: Modelling impacts of climate change on arable crop
665 diseases: progress, challenges and applications. Current Opinion in Plant Biology, 32,
666 101-109, 2016.
667 O'Brien, P., and Daigh, A.: Tillage practices alter the surface energy balance -A review.
668 Soil and Tillage Research, 195, 2019.
669 Penuelas, J., Rutishauser, T., and Filella, I.: Phenology Feedbacks on Climate Change.
670 Science, 324(5929), 887-888, 2009.
671 Reynolds, M., Foulkes, J., Furbank, R., Griffiths, S., King, J., Murchie, E., et al.:
672 Achieving yield gains in wheat. Plant Cell and Environment, 35(10), 1799-1823, 2012.
673 Richardson, A. D., Keenan, T. F., Migliavacca, M., Ryu, Y., Sonnentag, O., and Toomey,
674 M.: Climate change, phenology, and phenological control of vegetation feedbacks to the
675 climate system. Agricultural and Forest Meteorology, 169, 156-173, 2013.
676 Sacks, W. J., Deryng, D., Foley, J. A., and Ramankutty, N.: Crop planting dates: an
677 analysis of global patterns. Global Ecology and Biogeography, 19(5), 607-620, 2010.
678 Sacks, W. J., and Kucharik, C. J.: Crop management and phenology trends in the US
679 Corn Belt: Impacts on yields, evapotranspiration and energy balance. Agricultural and
680 Forest Meteorology, 151(7), 882-894, 2011.
681 Schillinger, W. F.: Rainfall Impacts Winter Wheat Seedling Emergence from Deep
682 Planting Depths. Agronomy Journal, 103(3), 730, 2011.

Sellers, P. J., Tucker, C. J., Collatz, G. J., Los, S. O., Justice, C. O., Dazlich, D. A., et al.: A Revised Land Surface Parameterization (SiB2) for Atmospheric GCMS. Part II: The Generation of Global Fields of Terrestrial Biophysical Parameters from Satellite Data. Journal of Climate, 9(4), 706-737, 1996.
Seneviratne, S. I., Corti, T., Davin, E. L., Hirschi, M., Jaeger, E. B., Lehner, I., et al.: Investigating soil moisture–climate interactions in a changing climate: A review. Earth-Science Reviews, 99(3), 125-161, 2010.
Seneviratne, S. I., Phipps, S. J., Pitman, A. J., Hirsch, A. L., Davin, E. L., Donat, M. G., et al.: Land radiative management as contributor to regional-scale climate adaptation and mitigation. Nature Geoscience, 11(2), 88-96, 2018.
Shi, P., Sun, s., Wang, M., Li, N., Wang, J., Jin, Y., et al.: Climate change regionalization in China (1961 - 2010)(In Chinese). Science China: Earth Sciences, 44(10), 2294-2306, 2014.
Song, Y., Jain, A. K., and McIsaac, G. F.: Implementation of dynamic crop growth processes into a land surface model: evaluation of energy, water and carbon fluxes under corn and soybean rotation. Biogeosciences, 10(12), 8201-8201, 2013.
Tao, F., Yokozawa, M., and Zhang, Z.: Modelling the impacts of weather and climate variability on crop productivity over a large area: A new process-based model development, optimization, and uncertainties analysis. Agricultural and Forest Meteorology, 149(5), 831-850, 2009.
Tao, F. L., Zhang, S., Zhang, Z., and Rotter, R. P.: Maize growing duration was prolonged across China in the past three decades under the combined effects of temperature, agronomic management, and cultivar shift. Global Change Biology, 20(12), 3686-3699, 2014.
Tao, F. L., Zhang, S. A., and Zhang, Z.: Spatiotemporal changes of wheat phenology in China under the effects of temperature, day length and cultivar thermal characteristics. European Journal of Agronomy, 43, 201-212, 2012.
Wuest, S. B.: Tillage depth and timing effects on soil water profiles in two semiarid soils. Soil Science Society of America Journal, 74(5), 1701-1711, 2010.
Wutzler, T., Lucas-Moffat, A., Migliavacca, M., Knauer, J., Sickel, K., Šigut, L., et al.: Basic and extensible post-processing of eddy covariance flux data with REddyProc. Biogeosciences, 15(16), 5015-5030, 2018.
Xiao, D. P., Moiwo, J. P., Tao, F. L., Yang, Y. H., Shen, Y. J., Xu, Q. H., et al.: Spatiotemporal variability of winter wheat phenology in response to weather and climate variability in China. Mitigation and Adaptation Strategies for Global Change, 20(7), 1191-1202, 2015.
Xiao, D. P., and Tao, F. L.: Contributions of cultivars, management and climate change to winter wheat yield in the North China Plain in the past three decades. European Journal of Agronomy, 52, 112-122, 2014.
Xiao, D. P., Tao, F. L., Liu, Y. J., Shi, W. J., Wang, M., Liu, F. S., et al.: Observed changes in winter wheat phenology in the North China Plain for 1981-2009. International Journal of Biometeorology, 57(2), 275-285, 2013.
Yuan, L., Wang, E., Yang, X., and Jing, W.: Contributions of climatic and crop varietal changes to crop production in the North China Plain, since 1980s. Global Change Biology, 16(8), 2287-2299, 2010.

728 Zhang, X., Huang, G., Huang, Z., Bian, X., and Jiang, X.: Effects of low temperature on
729 freezing injury of various winter wheat cultivars at different sowing time. Agricultural
730 Science & Technology, 13(11), 2332-2337, 2012.
731 Zhang, X., Tang, Q., Zheng, J., Ge, Q., and Mao, R.: Suppression of spring rain by
732 surface greening over North China Plain. International Journal of Climatology, 35(10),
733 2752-2758, 2015.
734 Zhang, X. Z., Tang, Q. H., Zheng, J. Y., and Ge, Q. S.: Warming/cooling effects of
735 cropland greenness changes during 1982-2006 in the North China Plain. Environmental
736 Research Letters, 8(2), 2013.
737